Research Article
Molecular and Cell Biology

JOURNAL
OF HEPATOLOGY

Nucleotide-binding oligomerization domain 1 (NOD1) modulates liver ischemia reperfusion through the expression adhesion molecules

Graphical abstract

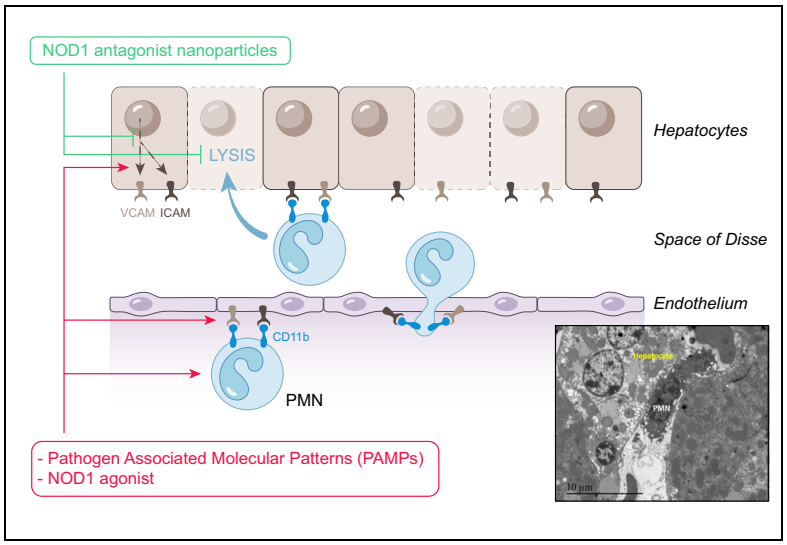

Highlights

- NOD1 agonists induced expression of adhesion molecules in the normal and IR-injured livers.
- NOD1 mediates interactions between hepatocytes and polymorphonuclear neutrophils during liver IR.
- Insoluble NOD1 inhibitors were efficiently integrated into PLGA nanoparticles for use *in vivo*.
- NOD1 antagonist nanoparticles reduced ICAM-1 expression and IR-induced liver injury.
- The NOD1 pathway modulates liver IR injury by targeting polymorphonuclear neutrophil function and adhesion molecules.

Authors

Guillaume Lassailly, Mohamed Bou Saleh, Natascha Leleu-Chavain, ..., Philippe Mathurin, Alexandre Louvet, Laurent Dubuquoy

Correspondence

guillaume.lassailly@chru-lille.fr
(G. Lassailly)
laurent.dubuquoy@inserm.fr
(L. Dubuquoy)

Lay summary

Nucleotide-binding oligomerization domain 1 (NOD1) is as an important modulator of polymorphonuclear neutrophil (PMN)-induced liver injury, which occurs in ischemia-reperfusion. Here, we show that the NOD1 pathway targets liver adhesion molecule expression on the endothelium and on hepatocytes through p38 and ERK signaling pathways. The early increase of adhesion molecule expression after reperfusion emphasizes the importance of adhesion molecules in liver injury. In this study we generated nanoparticles loaded with NOD1 antagonist. These nanoparticles reduced liver necrosis by reducing PMN liver infiltration and adhesion molecule expression.

http://dx.doi.org/10.1016/j.jhep.2019.01.019

Research Article
Molecular and Cell Biology

JOURNAL OF HEPATOLOGY

Nucleotide-binding oligomerization domain 1 (NOD1) modulates liver ischemia reperfusion through the expression adhesion molecules

Guillaume Lassailly[1,2,*], Mohamed Bou Saleh[1], Natascha Leleu-Chavain[1,3], Massih Ningarhari[1,2], Emilie Gantier[1], Rodolphe Carpentier[1], Florent Artru[1,2], Viviane Gnemmi[5], Benjamin Bertin[1], Patrice Maboudou[6], Didier Betbeder[1,4], Céline Gheeraert[7], François Maggiotto[1], Sébastien Dharancy[1,2], Philippe Mathurin[1,2], Alexandre Louvet[1,2], Laurent Dubuquoy[1,*]

[1]*LIRIC – Lille Inflammation Research International Center – U995, Univ. Lille, Inserm, CHU Lille, F-59000 Lille, France;* [2]*Service des Maladies de l'Appareil Digestif et de la Nutrition, CHU Lille, F-59000 Lille, France;* [3]*Institut de Chimie Pharmaceutique de Lille, Faculté de Pharmacie, Univ Lille, F-59000 Lille, France;* [4]*Université d'artois, F-62300 Lens, France;* [5]*Service d'anatomopathologie, CHU Lille, F-59000 Lille, France;* [6]*UF 8832 – Biochimie Automatisée, Pôle de Biologie Pathologie Génétique, CHRU de Lille, F-59000 Lille, France;* [7]*U1011 – EGID, Univ. Lille, Inserm, Institut Pasteur de Lille, F-59000 Lille, France*

Background & Aims: In liver transplantation, organ shortage leads to the use of marginal grafts that are more susceptible to ischemia–reperfusion (IR) injury. We identified nucleotide-binding oligomerization domain 1 (NOD1) as an important modulator of polymorphonuclear neutrophil (PMN)-induced liver injury, which occurs in IR. Herein, we aimed to elucidate the role of NOD1 in IR injury, particularly focusing on its effects on the endothelium and hepatocytes.

Method: *Nod1* WT and KO mice were treated with NOD1 agonists and subjected to liver IR. Expression of adhesion molecules was analyzed in total liver, isolated hepatocytes and endothelial cells. Interactions between PMNs and hepatocytes were studied in an *ex vivo* co-culture model using electron microscopy and lactate dehydrogenase levels. We generated NOD1 antagonist-loaded nanoparticles (np ALINO).

Results: NOD1 agonist treatment increased liver injury, PMN tissue infiltration and upregulated ICAM-1 and VCAM-1 expression 20 hours after reperfusion. NOD1 agonist treatment without IR increased expression of adhesion molecules (ICAM-1, VCAM-1) in total liver and more particularly in WT hepatocytes, but not in *Nod1* KO hepatocytes. This induction is dependent of p38 and ERK signaling pathways. Compared to untreated hepatocytes, a NOD1 agonist markedly increased hepatocyte lysis in co-culture with PMNs as shown by the increase of lactate dehydrogenase in supernatants. Interaction between hepatocytes and PMNs was confirmed by electron microscopy. In a mouse model of liver IR, treatment with np ALINO significantly reduced the area of necrosis, aminotransferase levels and ICAM-1 expression.

Conclusion: NOD1 regulates liver IR injury through induction of adhesion molecules and modulation of hepatocyte-PMN interactions. NOD1 antagonist-loaded nanoparticles reduced liver IR injury and provide a potential approach to prevent IR, especially in the context of liver transplantation.

Lay summary: Nucleotide-binding oligomerization domain 1 (NOD1) is as an important modulator of polymorphonuclear neutrophil (PMN)-induced liver injury, which occurs in ischemia-reperfusion. Here, we show that the NOD1 pathway targets liver adhesion molecule expression on the endothelium and on hepatocytes through p38 and ERK signaling pathways. The early increase of adhesion molecule expression after reperfusion emphasizes the importance of adhesion molecules in liver injury. In this study we generated nanoparticles loaded with NOD1 antagonist. These nanoparticles reduced liver necrosis by reducing PMN liver infiltration and adhesion molecule expression.

Introduction

In the field of liver transplantation, organ shortage is a major issue; especially in western countries where the living donor transplantation is still scare. This situation led transplant units to use of liver allografts following donation after cardiac death along with marginal and extended criteria donors.[1] These marginal grafts are known to be more susceptible to early graft dysfunction and retransplantation, increasing morbidity and mortality[2–5] mostly due to liver ischemia–reperfusion (IR) injuries.[6,7] Liver IR is a biphasic phenomenon in which hypoxia-induced lesions are exacerbated, after oxygen delivery is restored, by shear stress and tissue infiltration of polymorphonuclear neutrophils (PMNs).[8] This process of liver injury also occurs during hemodynamic instability and hepatic resection. It is a frequent cause of acute liver dysfunction.[2–5,9,10] Thus, preventing IR and its consequences remains a clinical challenge.

The pathophysiology of liver IR involves numerous cells (*i.e.* PMN, liver sinusoidal endothelial cells (LSECs) and hepatocytes) and is considered to be an experimental model of

Keywords: Liver ischemia reperfusion; Innate immunity; Liver transplantation; Adhesion molecules; Hepatocytes; Nanoparticles antagonist.
Received 10 July 2018; received in revised form 17 December 2018; accepted 2 January 2019; available online 25 January 2019

* Corresponding authors. Addresses: LIRIC – UMR995, 4e étage Est, Faculté de Médecine – Pôle Recherche, 1 Place Verdun, 59045 Lille Cedex, France. Tel.: +33 3 20974208, fax: +33 3 20623525 (L. Dubuquoy), or Service des Maladies de l'Appareil Digestif et de la Nutrition, Hôpital Huriez, CHU Lille, rue Michel Polonovski, 59045 Lille Cedex, France. Tel.: +33 3 20445321, fax: +33 3 20444713 (G. Lassailly).
E-mail addresses: guillaume.lassailly@chru-lille.fr (G. Lassailly), laurent.dubuquoy@inserm.fr (L. Dubuquoy).

PMN-mediated hepatitis.[3] The process of injury occurs during the reperfusion phase with PMN infiltration[11]. The first step of this event is the interaction between PMNs and the endothelium, allowing PMNs to enter the liver parenchyma. The upregulation of adhesion molecules (*i.e.* ICAM-1, VCAM-1, E-selectin) on LSECs follows reperfusion, allowing PMN recruitment in the rolling process,[12] through the binding of neutrophil adhesion molecules L-Selectin and Mac-1, an heterodimeric integrin (CDb/CD18).[13] The dual role and interactions between the endothelium and PMNs are accepted to be a cornerstone of the pathophysiology of liver IR. Thus, inhibiting adhesion molecule expression (such as ICAM, VCAM, E-selectin, CD44 and PECAM) or using blocking antibodies have been widely studied to reduce liver injury.[14]

Contrary to the endothelium, the mechanisms driving the interaction between PMNs and hepatocytes during liver IR remain to be clarified. The expression of adhesion molecules by the hepatocyte has been suggested to be important for its interaction with PMNs during IR.[15] Intercellular adhesion molecule-1 (ICAM-1) has been shown to be expressed on the plasma membrane of hepatocytes under IR conditions.[15] However, it remains unclear whether the regulation of ICAM expression on the hepatocyte impacts the severity of IR lesions.

There is evidence that damage-associated molecular patterns and pathogen-associated molecular patterns activate PMNs[16,17] leading to IR-mediated liver injury. We previously showed that activation of the nucleotide-binding oligomerization domain 1 (NOD1), a cytosolic pattern recognition receptor, was responsible for activation of PMN function and migration.[18] Indeed, by activating mitogen-activated protein (MAP) kinases such as p38, NOD1 leads to PMN infiltration in the liver, facilitating injury in a model of liver IR. At the opposite, *Nod1* knockout (KO) mice were protected against liver IR injury.[18] In addition, NOD1 is significantly expressed in the liver and in hepatocytes,[19] thus the NOD1 pathway appears to be a promising target for liver IR injury regulation.

The aim of our study was to dissect the role of the NOD1 pathway on the expression of adhesion molecules in the liver, and more specifically in endothelial cells and in hepatocytes. As IR lesions are induced by PMN liver parenchyma infiltration, we also explored the modulation of hepatocytes and PMN interaction by NOD1. Then, as proof of concept, we tested NOD1 as a potential therapeutic target for the prevention of IR lesions in a mouse model, by treating mice with a NOD1 inhibitor.

Materials and methods

Reagents

Three different NOD1 agonists were used in this study. The natural ligand iE-DAP (1 μg/ml *in vitro* and 5 mg/kg *in vivo*) and its derivative C12-iE-DAP (100 ng/ml *in vitro* and 3.3 mg/kg *in vivo*) were obtained from InvivoGen (Toulouse, France). FK565 (synthetic ligand, 10^{-6} M *in vitro* and 1 mg/kg *in vivo*) was obtained from Dr. M. Chamaillard. TNFα (50 ng/ml) and IFNγ (100 ng/ml) were obtained from R&D (Lille, France). We used ML-130 (Notilinib) and ALINO73 (analog of SB711[20]) synthetized by Natascha Leleu-Chavain as described as NOD1 antagonists.[20,21] The ERK inhibitor (U0126, Sigma, Saint-Quentin Fallavier, France) and p38 inhibitors (SB203580, InvivoGen, Toulouse France) were used at 10 μM. Resomer RG503H was used as a poly(lactic-co-glycolic acid) (PLGA) matrix (Evonik Industries AG, Deutschland) (Supplementary CTAT Table).

Animals

C57BL/6J wild-type mice (Janvier Labs, Le Genest-Saint-Isle, France), *Nod1* KO (C57BL/6J background)[18] and their wild-type littermates (*Nod1* WT) were used in this study. Animals were kept in a controlled environment (12 h light/dark cycles) and fed a standard rodent pellet diet (RM1, Special Diet Service, France) ad libitum. Experiments performed on animals were approved by the local ethics committee (n° 01757.01) in accredited facilities (n°B59-35010) according to government guidelines (n°2010/63/UE). Ethics committee number for animal experiments: n° 01757.01.

IR injury

We used a murine model of 70% partial hepatic ischemia for 60 min. Mice were or were not treated with a NOD1 agonist 24 h and 4 h before surgery. Then mice were anesthetized with 10 mg/kg xylazine and 100 mg/kg ketamine, and a midline laparotomy was performed. The left lateral and median lobes of the liver were ligatured using Ethicon mersutures™ F2541 (Ethicon, Issy Les Moulineaux, France). After 60 min of ischemia, the ligature was removed to initiate hepatic reperfusion. Mice were sacrificed 3 h (for hepatocyte isolation of the *ex vivo* experiment) or at 4, 8 and 20 h after reperfusion. Blood and liver samples were collected for analysis at each time point. Liver samples were fixed in paraformaldehyde 4% (w/v in PBS) and paraffin embedded or snap frozen.

Cell isolation and culture

PMNs were isolated following sterile peritonitis as previously described.[22] Briefly, mice received an intraperitoneal injection of 1 ml of a solution of oyster glycogen at 150 μg/μl in phosphate buffer saline (PBS). Mice were sacrificed 16 h later and peritoneal cells were harvested using 5 ml of sterile PBS without Ca^{2+}/Mg^{2+}. Exudate cells were determined to be >95% neutrophils by flow cytometry.

Hepatocytes were isolated by the collagenase perfusion method.[23] Briefly, mice were anesthetized with 2% isofluran. After laparotomy, the portal vein was cannulated (24G catheter, Terumo, Guyancourt, France). The liver was then perfused for 10 to 20 min at 5 ml/min with washing buffer (HBSS without Ca^{2+} Mg^{2+}, EDTA 0.5 mM, HEPES 50 mM), then perfused with collagenase buffer (HBSS without Ca^{2+} Mg^{2+}, HEPES 50 mM, $CaCl_2$ 50 mM, Collagenase type IV 0.0025% 850 CDU/mg (C5138, Sigma-Aldrich, Saint-Quentin Fallavier, France) for 6 min at 5 ml/min.

Following perfusion, the liver was collected in washing buffer and the Glisson's capsule was cut. Cell suspension was filtered in a 70 μM cell strainer. Cells were washed twice with washing buffer and centrifuged at 50 g for 2 min at room temperature to pellet murine hepatocytes. Hepatocytes were then washed with hepatocyte culture medium (DMEM Glutamax, glucose 4.5 g/L, Gentamycin 1%, FCS 10%, 10^{-7} M dexamethasone) and centrifuged at 500 g for 5 min. One million hepatocytes were plated in 6-well plate (Sarstedt, Marnay, France).

The main challenge to investigate the hepatocyte expression of adhesion molecules was to avoid any contamination of LSECs during the isolation of the mouse primary hepatocytes. To deal with this contingency, we have optimized our experimental method and checked the purity of isolated hepatocyte by FACS using CD31 as a marker for endothelial cell contamination. A purity >99% was considered acceptable (Fig. S1). In addition, a

cytospin followed by cell staining were performed before *in vitro* and *ex vivo* analysis to confirm purity.

Primary Human umbilical vein endothelial cells (HUVEC) were obtained from Prof. Eric Boulanger (Lille, France) and were maintained in endothelial cell basal medium supplemented with Bullet Kit (EBM-2) on a culture flask coated with 0.1% gelatin and maintained at 37 °C in a humidified atmosphere with 5% carbon dioxide. HUVECs cultured from passages 4 to 8 were used for the experiments.

Hepatocyte and PMN co-culture

Freshly isolated hepatocytes were plated on a 48-well plate (1.25×10^5 cell per well) and incubated at 37 °C with 5% CO_2 for 36 h. Purified peritoneal PMN (6.25×10^5 cell per well) were or were not added to the hepatocyte culture for 4 h in HBSS medium (without phenol red). Supernatants were then harvested and centrifuged at 500 g for 5 min to discard cells and debris. These supernatants were used to quantify lactate dehydrogenase (LDH) activity using the manufacturer's protocol (Roche, Boulogne-Billancourt, France).

Real-time PCR for mRNA quantification

Real-time PCR analyses were performed for quantification of mRNA expression. Mouse glyceraldehyde-3-phosphate-dehydrogenase (GAPDH) was used as a housekeeping gene. Sequence-specific PCR primers were designated using Primer3 Software;[24,25] see Table S1 and Supplementary CTAT Table for details). Total RNA was extracted from isolated hepatocytes or liver samples using Nucleospin®RNAII (Macherey-Nagel EURL, Hoerdt, France). First strand cDNA was synthesized from 1 μg total RNA using a High Capacity cDNA Reverse Transcription Kit (Applied Biosystems, Courtaboeuf, France). Real-time PCR was performed using Power SYBR Green PCR Master Mix (Applied Biosystems, Foster City, CA, USA) in StepOne plus (Applied Biosystems, Foster City, CA, USA).

Western blot

For western blot studies, proteins were extracted from liver samples or isolated hepatocytes in a lysis buffer including PBS with 1% Nonidet P40, 0.5% sodium deoxycholate, 0.1% sodium dodecyl sulphate (SDS), 100 mM Phenyl Methyl Sulfonyl Fluoride and a classical protease inhibitor cocktail (Roche Diagnostics, Penzberg, Germany) as well as phosphatase inhibitors (Sigma-Aldrich, Lyon, France). Fifty micrograms of total proteins were then separated by SDS-PAGE and electroblotted on nitrocellulose membranes. Membranes were incubated overnight with primary antibodies (see Table S2 and Supplementary CTAT Table for details). Immunodetection was completed with a secondary peroxidase-conjugated antibody (1:1,000, Dako Laboratories, Trappes, France) and chemiluminescence was performed according to the manufacturer's protocol (ECL, Amersham Pharmacia Biotech, Orsay, France). β-actin was used as a loading control. Band intensity was analyzed using the MM4000 Pro (CareStream, Noisy-le-Grand, France), quantified using Image J (NIH) and compared to β-actin. Results were expressed as relative units (RU).

Immunohistochemistry, necrosis area quantification & liver PMN quantification

Liver samples were fixed in paraformaldehyde (PFA) 4% and embedded in paraffin. Four-micrometer-thick sections were exposed to primary antibodies after a specific step of heat-performed antigen retrieval (see Table S2 for details) and then to a biotinylated secondary antibody for 1 h. After washing in TBS + 0.05% Tween 20, sections were incubated with strepavidin-horseradish peroxidase (Dako Laboratories, Trappes, France). Staining was revealed using 3,3′-diaminobenzidine substrate (Dako Laboratories) for 1 to 5 min before the reaction was stopped in distilled water, and counterstained with hematoxylin. Negative controls were incubated with irrelevant serum or isotype-matched immunoglobulin instead of the specific antibody. Stained slides were observed and analyzed under a microscope (Leica, Bensheim, Germany). Pictures were obtained using Axio Scan.Z1 (Zeiss, Göttingen, Germany).

Quantification of necrosis was obtained on digital images of IR livers (3 per mice) obtained from Axio Scan Z1 (Zeiss, Göttingen, Germany). The area of necrosis was defined as the ratio of (area of necrosis/ total liver area) × 100.

Quantification of PMN infiltration was performed by counting PMN on 8–10 fields of necrosis and/or centrolobular area (magnification, 400) for each mouse.

Human ICAM-1 promoter analysis

The proximal human *ICAM-1* promoter was amplified from human liver genomic DNA using the following primers: forward primer (5′-AGGGAGCTCTCGTCAAGATCCAAGCTAGCTG-3′) and (5′-GGAAGATCTGTGATCCTTTATAGCGCTAGCC-3′) corresponding to fragments between −895 and −57 upstream from ATG. The purified fragment was cloned in the multiple cloning site of the reporter plasmid pGL4.10 [luc2] (Promega, France) using SalI and BglII (NEB, USA). This construct (Prom ICAM, Fig. 5B) was amplified and purified before sequencing to confirm correct integration of the promoter. CV-1 cells (ATCC® CCL-70™) were plated in 48-well plates (40,000 cells/well) and transfected with empty pGL4.10 [luc2] or Prom ICAM (100 ng/well) and a human NOD1 expression vector (20 ng/well, pHA-NOD1 kind gift from Dana J. Philpott). After 20 h, cells were washed and lysed for luminescence quantification.

Nanoparticle synthesis, formulation and characterization

PLGA nanoparticles (np) were prepared as previously described.[26] The Resomer RG503H (10 mg) was dissolved in 1 ml of an organic phase consisting of acetone and ethanol (85:15). After complete dissolution of the Resomer, it was injected into 10 ml water by stirring for 30 min at room temperature (21 to 24 °C). Organic solvents were then evaporated with a rotary vacuum evaporator at 120 rpm, 28 °C for 4 min. The resulting nanoparticles are used as a control (np). Association with the NOD1 antagonist was performed by post-loading and adding the antagonists into the nanoparticle suspension. ML130 was dissolved in DMSO at 100 mg/ml and loaded with np from 0.075% to 3% (w/w) for *in vitro* cell delivery corresponding to treatment from 0.125 to 5 μM (NP-ML130). ALINO73 was dissolved in DMSO at 20 mg/ml and loaded with np from 0.2% to 4% (w/w) for *in vitro* cell delivery corresponding to treatment from 0.25 to 5 μM (npALINO). For *in vivo* delivery, ALINO73 was loaded at 7.5% (w/w NP) and 5% (w/v) of glucose was added to the final suspension to compensate for osmolarity.

The *in vivo* formulation of np ALINO was characterized for size (Z-Average = 92.8 nm) and zeta potential (−11.8 mV) respectively by dynamic light scattering and electrophoretic mobility analysis on a ZetaSizer NanoZS (Malvern Instrument, France). The poly dispersity index was 0.259.

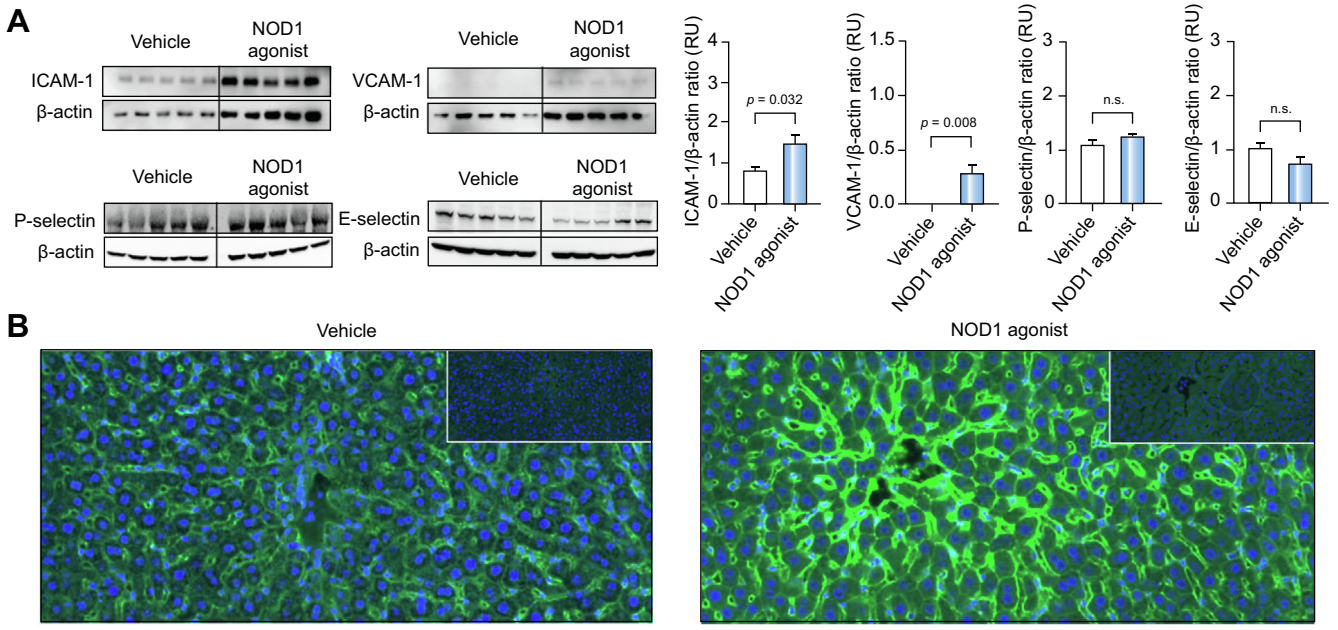

Fig. 1. NOD1 activation induced liver expression of adhesion molecules under physiological condition. (A) Representative western blot of livers extracted from C57BL/6 mice treated with vehicle or NOD1 agonist (FK565). ICAM-1, VCAM-1, P-selectin and E-selectin protein expression were compared to β-actin. Right panel histograms represent ratio of band intensity of the adhesion molecules compared to β-actin. Statistical test: Mann-Whitney *U*, significance is defined by $p < 0.05$. Statistical significance is indicated. (B) Representative ICAM-1 immunostainings of livers extracted from mice only treated with vehicle (left panel) or NOD1 agonist (iE-DAP) (right panel). Negative controls are included (upper right corner). Livers from vehicle-treated mice displayed significant staining on sinusoids. After NOD1 agonist treatment, sinusoidal staining was reinforced and a marked staining was observed on hepatocytes. RU, relative units.

Statistics

Data were expressed as medians, means ± SEM or means ± SD. All comparisons were analyzed using the Mann-Whitney *U* test. Statistics were calculated using GraphPad Prism version 5.0, (GraphPad Software, San Diego, CA, USA). Differences were considered to be statistically significant if p was <0.05.

Results

Induction of adhesion molecule expression in livers of mice treated with NOD1 agonists, in normal condition (without liver IR)

Twenty hours after administering a NOD1 agonist injection under normal conditions (without liver IR), mouse livers displayed a significant induction of 2 important adhesion molecules, ICAM-1 and VCAM-1, (1.4 RU *vs.* 0.8 RU, $p = 0.032$ and 0.25RU *vs.* 0.00 RU, $p = 0.008$ respectively), compared to vehicle-treated mice. There was no effect of NOD1 agonist on E-selectin and P-selectin protein expression (Fig. 1A). The immunostaining of ICAM-1 showed that NOD1 agonist treatment increased ICAM-1 expression not only on the endothelium but also on hepatocyte membranes compared to untreated livers which mainly displayed endothelial staining (Fig. 1B).

NOD1 agonist increases liver IR injury and upregulates ICAM-1 and VCAM-1

Twenty hours after IR, the livers of mice treated with the NOD1 agonist displayed a larger necrosis area than those treated with vehicle (Fig. 2A). The kinetic analysis of PMN infiltration in liver parenchyma revealed that, regardless of NOD1 treatment, there was no PMN infiltration 4 h after reperfusion. It became significant 8 h after reperfusion. At 8 and 20 h after reperfusion, NOD1 agonist treatment significantly induced PMN liver infiltration compared to vehicle treatment. Additionally, keratinocyte chemoattractant (KC) expression was upregulated 20 h after reperfusion in livers treated with the NOD1 agonist. (Fig. 2B)

Four hours after reperfusion, aminotransferases increased (aspartate aminotransferase [AST] 2,078 ± 350 IU/L *vs.* 1,921 ± 346.5 IU/L and alanine aminotransferase [ALT] 2,885 ± 547.7 IU/L *vs.* 2,610 ± 385 IU/L) without differences between the 2 treatment conditions (NOD1 agonist *vs.* vehicle). ALT levels increased after 8 h of reperfusion, and were significantly higher in the NOD1 agonist group (3,910 ± 25 IU/L *vs.* 3,139.6 ± 292.5 IU/L; $p = 0.05$) whereas AST levels were not different in each group (1,802.0 ± 137.3 IU/L *vs.* 1,905 ± 159.6 IU/L). After 20 h of reperfusion, the NOD1 agonist conditions presented significantly higher values of aminotransferases than vehicle conditions (AST 3,173 ± 96 IU/L *vs.* 2,402 ± 109 IU/L; $p < 0.01$ and ALT 4,627 ± 78 IU/L *vs.* 3,062 ± 52 IU/L; $p < 0.01$) (Fig. 2C).

NOD1 agonist treatment upregulated *Icam-1* and *Vcam-1* mRNA expression at an early time point after reperfusion (4 h) (Fig. 2D). This mRNA overexpression began before PMN infiltration and the establishment of histological necrosis (Fig. S2). At a protein level, ICAM-1 and VCAM-1 were significantly induced 20 h after reperfusion in mice treated with NOD1 agonist (ICAM-1: 1.8 to 2.6 RU; $p = 0.049$ and VCAM-1: 0.37 to 0.94 RU; $p = 0.049$) (Fig. 2E).

Considering other adhesion molecules, there was no difference of expression after NOD1 agonist treatment in liver IR condition for E-selectin and P-selectin ($p < 0.05$) (Fig. 2E).

NOD1 pathway targets ICAM-1 and VCAM-1 expression *in vitro* in primary endothelial cells and hepatocytes

HUVECs were cultured and exposed to NOD1 agonist at different dosages (0, 0.1 and 1 μg). The mRNA expression of *Icam-1,*

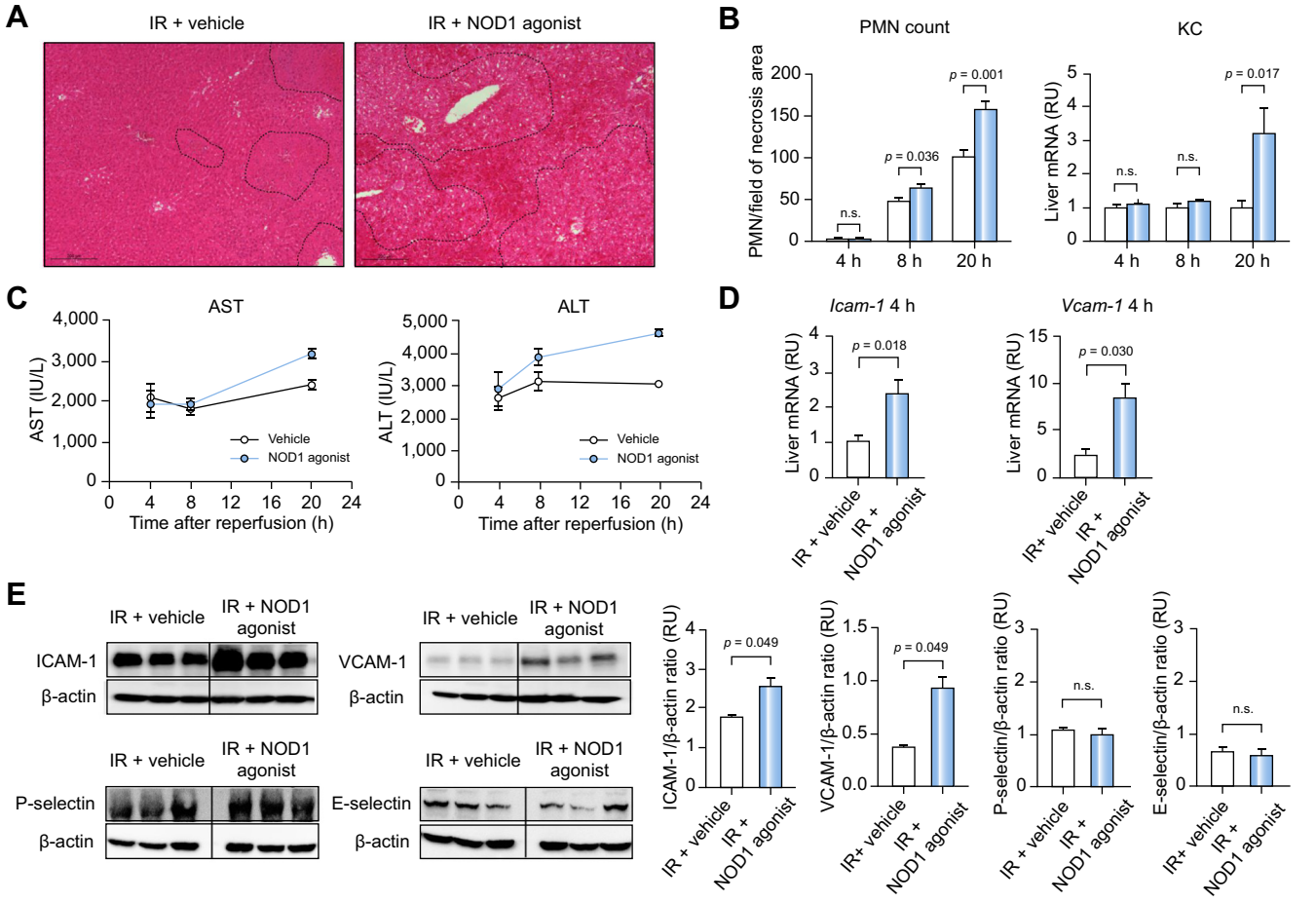

Fig. 2. NOD1 activation induced liver expression of adhesion molecules after liver IR. (A) Representative H&E histological picture of livers extracted from C57BL/6 mice that underwent IR and were treated with vehicle (IR + Vehicle, left panel) or NOD1 agonist (iE-DAP) (IR + NOD1 agonist, right panel). Dashed lines circle areas of liver injury. (B) Histograms representing liver PMN count and relative expression of liver KC mRNA 4, 8 and 20 h after reperfusion in C57BL/6 mice treated with vehicle (IR + Vehicle, white bars) or NOD1 agonist (IR + NOD1 agonist, blue bars). Results are expressed as mean ± SEM. Statistical test: Mann-Whitney *U*, significance is defined by $p < 0.05$. Statistical significances are indicated. (C) Kinetic determination of AST (left panel) and ALT (right panel) in C57BL/6 mice serum 4, 8 and 20 h after reperfusion and treatment with vehicle (grey line) or NOD1 agonist (blue line). Results are expressed as mean ± SEM. Statistical test: Mann-Whitney *U*, significance is defined by $p < 0.05$. Statistical significances are indicated. (D) Histograms representing early (4 h after reperfusion) liver expression of *Icam-1* and *Vcam-1* mRNA in C57BL/6 mice treated with vehicle (IR + Vehicle, white bars) or NOD1 agonist (IR + NOD1 agonist, blue bars). Results are expressed as mean ± SEM. Statistical significances are indicated. Statistical test: Mann-Whitney *U*, significance is defined by $p < 0.05$. (E) Representative western blot of liver extracted 20 h after reperfusion from C57BL/6 mice treated with vehicle (IR + Vehicle) or NOD1 agonist (IR + NOD1 agonist). Protein expression of ICAM-1, VCAM-1, P-selectin and E-selectin was compared to β-actin. Lower panel histograms represent the ratio of band intensity of the adhesion molecules compared to β-actin. Statistical test: Mann-Whitney *U*, significance is defined by $p < 0.05$. Statistical significance is indicated. ALT, alanine aminotransferase; AST, aspartate aminotransferase; IR, ischemia reperfusion; KC, keratinocyte chemoattractant; PMN, polymorphonuclear neutrophil; RU, relative units.

Vcam-1 and *E-selectin* were induced by NOD1 agonist treatment in a dose-dependent manner. However, *Pecam* mRNA expression was not significantly modified by NOD1 activation (Fig. 3A).

Mouse primary hepatocytes were cultured *in vitro*. Before analysis, the purification of isolated cells was confirmed (hepatocyte purity >99%, Fig. S1). Primary hepatocytes were then exposed to NOD1 agonists under basal or inflammatory (TNF/IFN) conditions. As shown in Fig. 3B, *Icam-1* mRNA was induced twice in *Nod1* WT hepatocytes treated with the NOD1 agonist, as well as under inflammatory conditions induced by TNF/IFN. *Vcam-1* mRNA was significantly induced by NOD1 activation (1.2 RU *vs.* 3.3 RU, $p = 0.005$, Fig. 3A). Induction of *Icam-1* and *Vcam-1* mRNA expression was synergistic with the NOD1 agonist and TNF/IFN treatments (Fig. 3B). These data were confirmed at the protein level in mouse primary isolated hepatocytes which showed that ICAM-1 and VCAM-1 were significantly increased by the NOD1 agonist both under basal and inflammatory conditions (Fig. 3D). To confirm the specificity of the NOD1 agonist, hepatocytes were isolated from *Nod1* KO mice and exposed to NOD1 agonist treatment under basal and inflammatory conditions. Real-time PCR and western blot showed that the NOD1 agonist did not induce ICAM-1 and VCAM-1 in *Nod1* KO hepatocytes but responded to TNF/IFN treatment (Fig. 3C,E).

NOD1 pathway targets ICAM-1 and VCAM-1 expression *ex vivo* in hepatocyte

In *ex vivo* conditions, NOD1 agonist treatment of sham-operated mice induced significant hepatocyte expression of *Icam-1* and *Vcam*-1 mRNA (6-fold and 10-fold increase, respectively) compared to vehicle-treated animals (Fig. 4A). IR alone also induced *Icam-1* and *Vcam-1* mRNA (4-fold and 5-fold increase, respectively). NOD1 activation during IR markedly increased

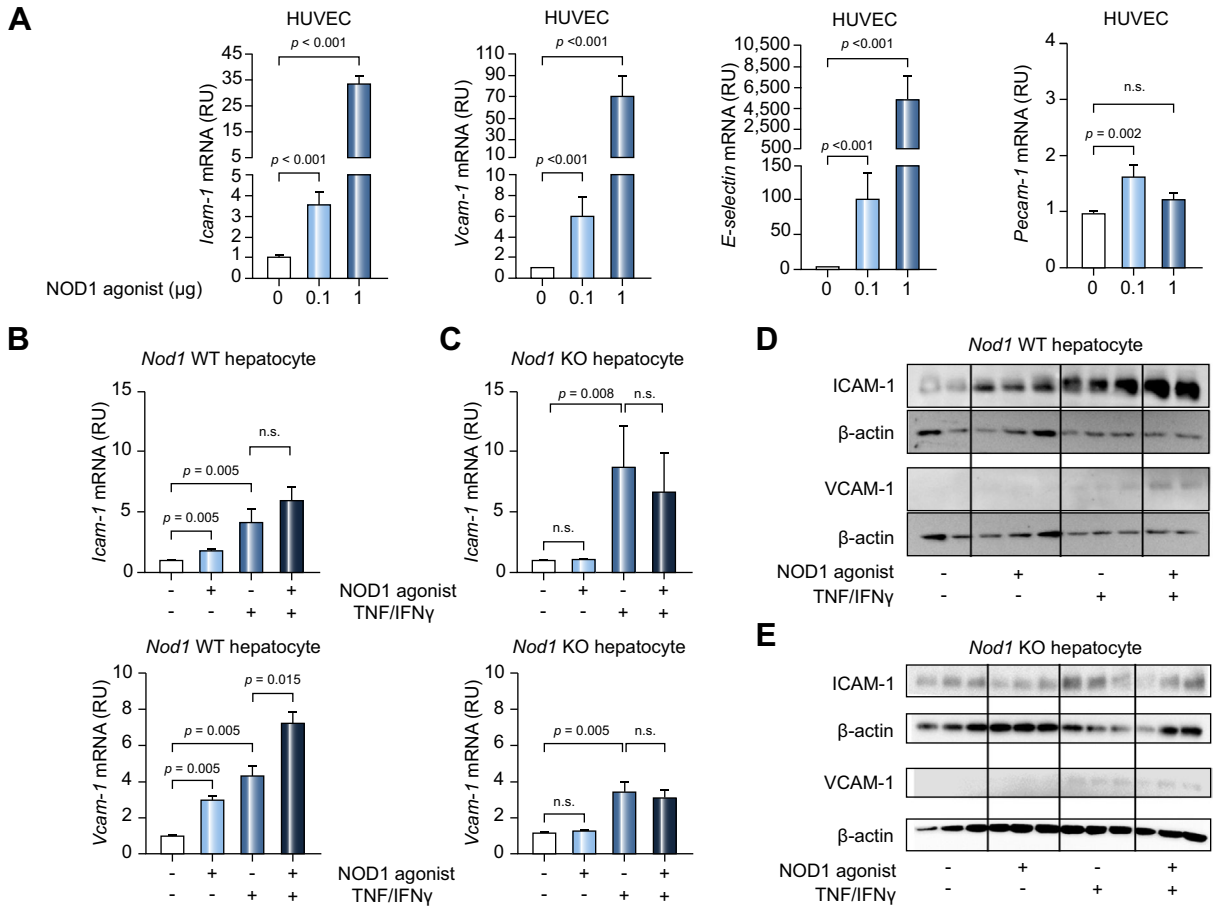

Fig. 3. NOD1 activation induces hepatocyte expression of ICAM-1 and VCAM-1. (A) mRNA expression of *Icam-1*, *Vcam-1*, *E-selectin* and *Pecam* in HUVECs, Statistical test: Mann-Whitney *U*, significance is defined by $p < 0.05$. (B,C) mRNA expression of *Icam-1* (upper panel) and *Vcam-1* (lower panel) in primary hepatocytes isolated from *Nod1* KO mice (C) or their WT littermates (*Nod1* WT mice, B). Cells were treated with vehicle or NOD1 agonist (FK565) and/or TNF 50 ng/ml and IFNγ 100 ng/ml (TNF/IFNγ). Statistical significance was indicated. Statistical test: Mann-Whitney *U*, significance is defined by $p < 0.05$. (D,E) Representative western blots for quantification of ICAM-1 (upper blot) and VCAM-1 (lower blot) protein expression that were compared to β-actin. (C,D) Primary hepatocytes isolated from *Nod1* KO mice (D) or their wild-type littermates (*Nod1* WT mice, C), were treated with vehicle or a NOD1 agonist (FK565) and/or TNF 50 ng/ml and IFNγ 100 ng/ml (TNF/IFNγ). Statistical test: Mann-Whitney *U*, significance is defined by $p < 0.05$. Statistical significance is indicated. HUVECs, human umbilical vein endothelial cells; KO, knockout; RU, relative units; WT, wild-type.

hepatocyte *Icam-1* and *Vcam-1* mRNA expression (25-fold and 20-fold increase, respectively) compared to vehicle-treated sham animals (Fig. 4A). At the protein level, NOD1 agonist treatment in sham-operated mice strongly induced hepatocyte expression of ICAM-1 and VCAM-1 (7.1-fold and 4.0-fold, respectively, Fig. 4C) compared to untreated mice. After 3 h of reperfusion, induction of the ICAM-1 and VCAM-1 proteins also increased significantly (2.1-fold and 2.0-fold respectively, Fig. 4C). NOD1 agonist-treated *Nod1* WT mice that underwent liver IR showed massive induction of hepatocyte expression of ICAM-1 and VCAM-1 protein (37-fold and 109-fold, respectively) compared to vehicle-treated sham animals. More importantly, NOD1 agonist treatment increased ICAM-1 and VCAM-1 protein expression by 17.7 and 54.5-fold respectively upon liver IR conditions (Fig. 4C).

In *Nod1* KO mice, the NOD1-mediated induction of ICAM-1 and VCAM-1 expression was blunted both following IR or a sham-operation (Fig. 4B,D).

NOD1 activation in hepatocytes amplifies the interaction with PMNs and subsequent lysis

Examination of the co-culture by electron microscopy revealed important adhesion of PMNs on hepatocytes which showed signs of distress such as swelling of mitochondria, cytoplasm clarification and lysosome (Fig. 5A).

Hepatocytes isolated from *Nod1* WT mice that were or were not treated with a NOD1 agonist showed low levels of spontaneous lysis when cultured alone (Fig. 5B). A significant increase in LDH activity was observed when hepatocytes from untreated mice were co-cultured with PMN isolated from untreated WT mice. When hepatocytes from NOD1 agonist-treated mice were co-cultured with PMN isolated from untreated WT mice, there was a significant increase in LDH activity compared to hepatocytes from vehicle-treated animals (Fig. 5B).

To confirm the specificity of NOD1 in relation to this event, we reproduced these experiments with hepatocytes isolated from *Nod1* KO mice treated or not with a NOD1 specific agonist. As observed in Fig. 5C, targeting of *Nod1* KO hepatocytes by PMN was reduced and NOD1 agonist-induced lysis was completely blunted.

NOD1 signaling pathways driving ICAM-1 and VCAM-1 expression in hepatocytes

A liver active form of ERK (phospho ERK) was induced from 10 to 30 min after treatment with a NOD1 agonist (Fig. 6A). A similar pattern was observed for p38 since active phospho p38 was

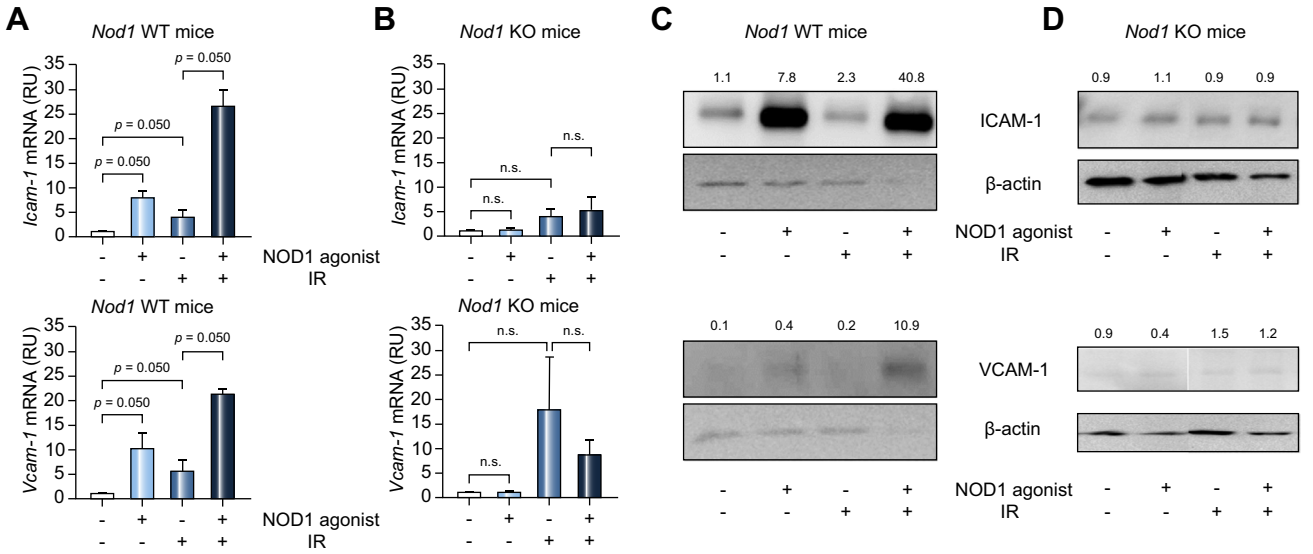

Fig. 4. During ischemia reperfusion, NOD1 pathway induced hepatocyte expression of adhesion molecules. (A,B) *Ex vivo* mRNA expression of *Icam-1* (upper panel) and *Vcam-1* (lower panel) in primary hepatocytes isolated from *Nod1* KO mice (B) or their wild-type littermates (*Nod1* WT mice, A). Mice were treated or not with NOD1 agonist (FK565) after sham surgery or IR. Statistical test: Mann-Whitney *U*, significance is defined by $p < 0.05$. Statistical significance is indicated. (C,D) Representative western blots for quantification of ICAM-1 (upper blot) and VCAM-1 (lower blot) protein expression that were compared to β-actin in *ex vivo* primary hepatocytes. *Nod1* KO mice (D) or their wild-type littermates (*Nod1* WT mice, C), were treated or not with a NOD1 agonist (FK565) after sham surgery or IR. Ratios of band intensity are indicated as RU. IR, ischemia reperfusion; KO, knockout; RU, relative units; WT, wild-type.

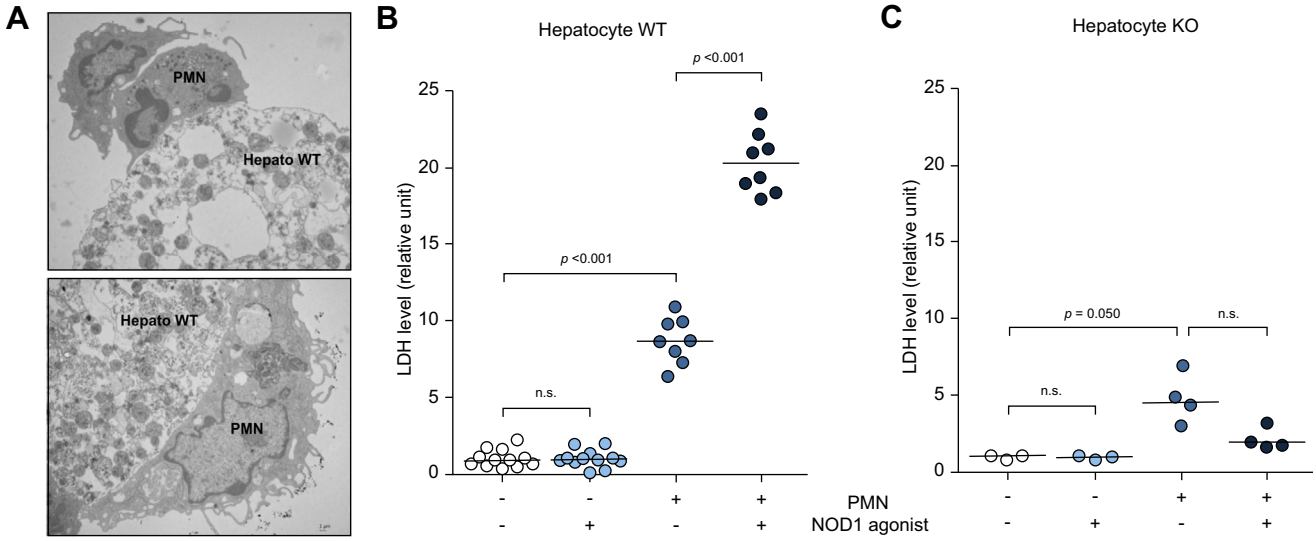

Fig. 5. NOD1 pathway activation leads to hepatocyte lysis by neutrophils. Co-culture experiments to assess hepatocyte (Hepato) and neutrophil (PMN) interaction and cell lysis. (A) Representative cytology formed by electronic microscopy of the interaction between neutrophils (PMN) and hepatocytes (Hep). (B) Primary hepatocytes were isolated from wild-type mice (Hepato WT) treated or/not with a NOD1 agonist (FK565). Then hepatocytes were co-cultured (or not) with PMN harvested from WT mice. Dosage of LDH in co-culture supernatants (RU). (C) Primary hepatocytes were isolated from *Nod1* KO mice (Hepato KO) treated or/not with a NOD1 agonist (FK565). Then hepatocytes were co-cultured (or not) with PMN harvested from WT mice. Dosage of LDH in co-culture supernatants (RU). Statistical test: Mann-Whitney *U*, significance is defined by $p < 0.05$. KO, knockout; PMN, polymorphonuclear neutrophil; RU, relative units; WT, wild-type.

induced at 10 and 30 min and then returned to the steady state 60 min after stimulation with a NOD1 agonist (Fig. 6B). Treatment with the ERK inhibitor (U0126) significantly limited the increase in *Icam-1* and significantly blocked the *Vcam-1* mRNA overexpression induced by the NOD1 agonist (Fig. 6C-D). The p38 inhibitor (SB203580) further blocked NOD1-induced hepatocyte *Icam-1* and *Vcam-1* mRNA expression. Co-treatment with both ERK and p38 inhibitors did not increase blockade of the NOD1 effect.

In vitro, we first cloned the human *ICAM-1* promoter (Fig. 6E) and showed that NOD1 activation by an agonist resulted in a 50% increase in luciferase activity driven by this promoter compared to untreated cells (Fig. 6F).

NOD1 antagonist development to prevent IR-induced liver injury

ML130 and ALINO73 are 2 specific NOD1 inhibitors that have been identified by screening different libraries of chemical

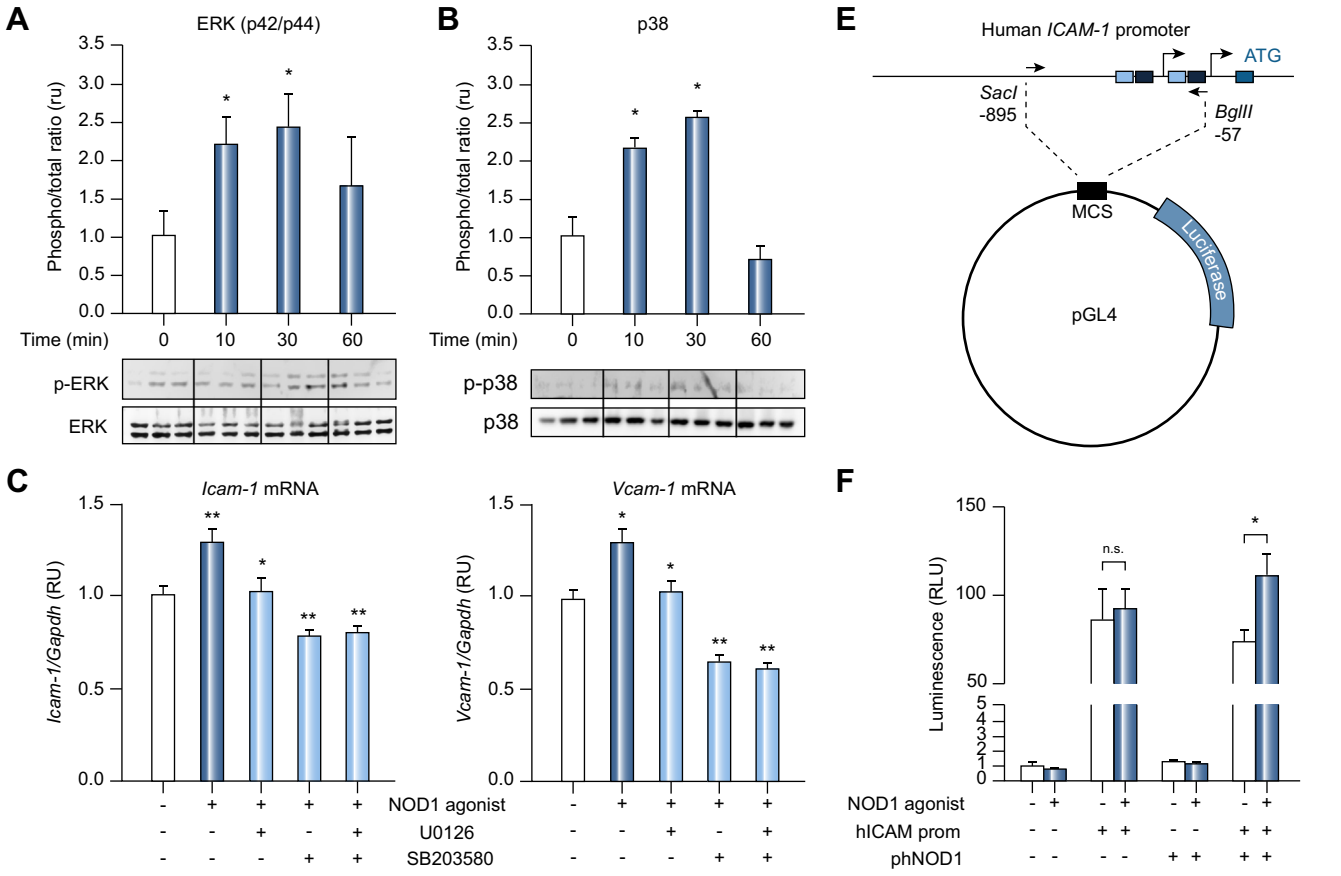

Fig. 6. NOD1 signaling and ICAM-1 promoter. (A,B) Ratio of band intensity of phospho MAP kinases compared to total MAP kinases from western blots performed on liver extracts from C57BL/6 mice 0, 10, 30, 60 min after treatment with a NOD1 agonist (iE-DAP). Mean ± SD are represented (n = 6) and statistical significance is indicated as $^{*}p$ <0.05 as compared to baseline (time point 0 min). The lower panel corresponds to representative western blot. (A) Liver ERK (p42/p44) activation. (B) Liver p38 activation. Statistical test: Mann-Whitney *U*, significance is defined by p <0.05. (C,D) Histograms for mRNA expression of *Icam-1* (C) and *Vcam-1* (D) in hepatocytes treated or not with a NOD1 agonist (iE-DAP) and with an ERK inhibitor (U0126, 10 μM) and/or a p38 inhibitor (SB203580, 10 μM). Results are expressed as RU (mean ± SEM, n = 5–10). Statistical significance is indicated as $^{*}p$ <0.05 or $^{**}p$ <0.01. Untreated control (white bar) was compared to positive control (NOD1 agonist treatment, dark blue). Inhibitor treated cells (light blue bars) were compared to positive control (dark blue bar). Statistical test: Mann-Whitney *U*, significance is defined by p <0.05. (E) Schematic diagram representing 838 base pairs of the human *ICAM*-1 promoter been cloned in the reporter vector, pGL4. NF-κB response element (black boxes) and AP-1 (blue boxes) response elements are indicated. Transcription starts are represented as () and ATG is indicated as a purple box. (F) CV-1 cells are transfected or not with human NOD1 expression vector (phNOD1) and transfected or not with a reporter vector containing human *ICAM-1* promoter (hICAM prom). Cells with different transfection conditions are treated or not with a NOD1 agonist (C12-iE-DAP). The human *ICAM-1* promoter activity is evaluated using luminescence and quantified as relative light units. Statistical significance is indicated as *. Statistical test: Mann-Whitney *U*, significance is defined by p <0.05.

compounds for activation or inhibition of NOD receptors.[20,21] In an *in vitro* model that allows evaluation of NOD1 activation, cells were treated with a NOD1 agonist and increasing doses of either ML130 or ALINO73 (Fig. S3A-B). Treatment with a NOD1 agonist-induced significant expression of the reporter gene (SEAP, OD_{655} 0.165 ± 0.014). Addition of ML130 resulted in a dose-dependent decrease in NOD1 activity from 0.16 μM (OD_{655} 0.106 ± 0.014) to maximum inhibition at 5 μM (OD_{655} 0.013 ± 0.014). Treatment with ALINO73 led to dose-dependent inhibition of NOD1 activity from 0.16 μM (OD_{655} 0.197 ± 0.020 *vs.* 0.140 ± 0.021) to maximum inhibition at 2.5 μM (OD_{655} 0.030 ± 0.014).

Because both NOD1 antagonists are not soluble in injectable vehicles used for *in vivo* applications, ML130 and ALINO73 were associated with PLGA nanoparticles to facilitate *in vivo* delivery to the liver.

The effect of antagonist-loaded nanoparticles on NOD1 activity was tested in the same *in vitro* system as above (Fig. S3C-D). As shown in Fig. S3C when ML130 was associated with PLGA nanoparticles, it lost its inhibitory potential on NOD1 activity, ALINO73-loaded nanoparticles (np ALINO) appeared to be at least as effective as free ALINO73 for the dose-dependent inhibition of NOD1 activity *in vitro* (Fig. S3D).

Modulating IR-induced liver injury with NOD1 antagonist nanoparticles

np ALINO was then used to test the *in vivo* potential of NOD1 antagonists. Mice received an intravenous injection of nanoparticles that was either empty (np Empty) or loaded with the NOD1 inhibitor (np ALINO) before undergoing 1 h of ischemia. As shown in Fig. 7A, mice treated with np Empty displayed large areas of IR-induced necrosis. However, when treated with the np ALINO the area of necrosis was lower in mouse livers (26.0 ± 3.2% *vs.* 15.6 ± 2.9%, p = 0.038) (Fig. 7B-C). These results were confirmed by determining serum aminotransferase. After treatment with np ALINO, serum ALT significantly decreased compared to treatment with empty nanoparticles (3,935 ± 493 IU/L *vs.* 5,814 ± 615 IU/L, p = 0.040) (Fig. 7D). This

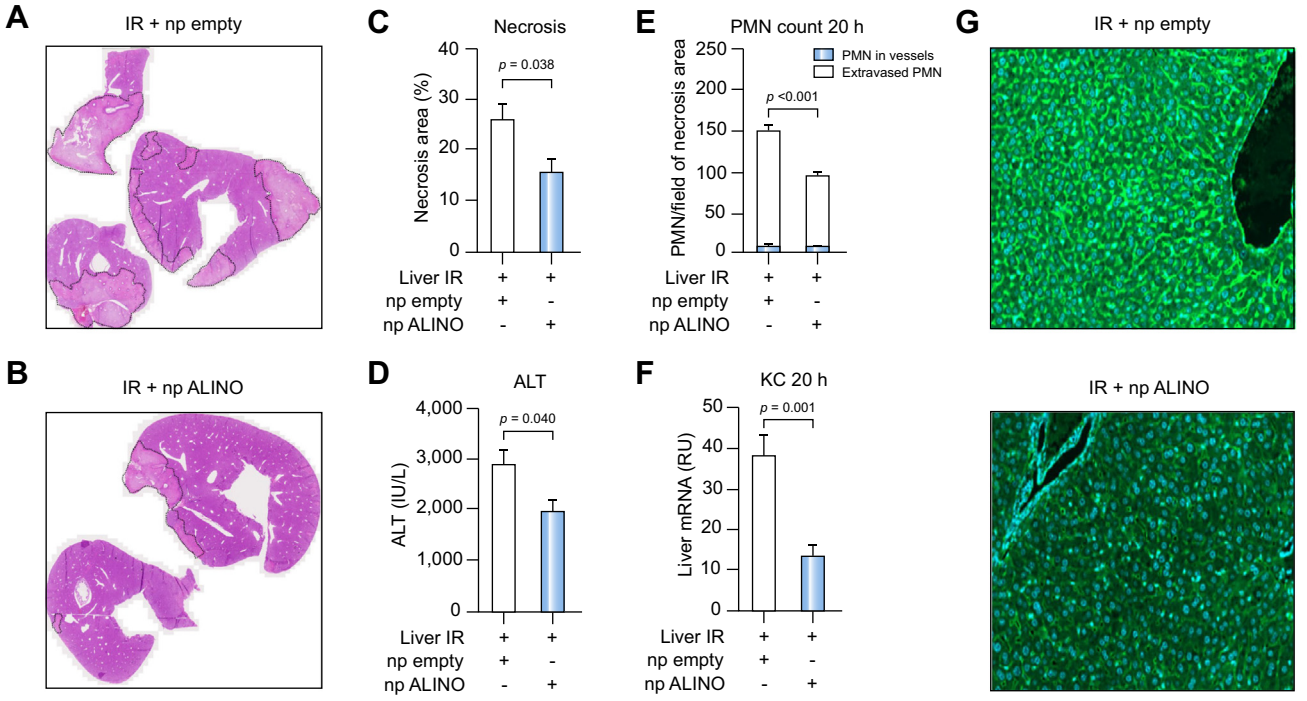

Fig. 7. Use of antagonists to target NOD1 in liver. C57BL/6 mice received an intravenous injection of empty (np Empty) or ALINO73-loaded nanoparticles (np ALINO) with a dose corresponding to 5 mg/kg of ALINO73. n = 13 in each group. Six hours later mice underwent 60 min of ischemia and 20 h of reperfusion. (A, B) Image of mouse liver histology (H&E staining) following IR injury. (A) Liver from mouse that underwent IR and treated with empty PLGA nanoparticles (IR + np Empty) display large injury areas (surrounded by dotted lines). (B) Liver from mouse that underwent IR and treated with ALINO73-loaded nanoparticles (IR + np ALINO). Injury areas are obviously more limited. (C) Quantification of liver necrotic areas from mice that underwent IR (Liver IR) before treatment with empty PLGA nanoparticles (np Empty) and from mice that underwent IR before treatment with ALINO73-loaded nanoparticles (np ALINO). Results are expressed in percentage of necrotic surface among total liver surface as mean ± SEM. Statistical test: Mann-Whitney *U*, significance is defined by $p < 0.05$. (D) Serum ALT from mouse that underwent IR (Liver IR) before treatment with empty PLGA nanoparticles (np Empty) and from mouse that underwent IR before treatment with ALINO73-loaded nanoparticles (np ALINO). Statistical significances are indicated. Statistical test: Mann-Whitney *U*, significance is defined by $p < 0.05$. (E) Histogram representing liver PMN count 20 h after reperfusion (Liver IR) in mice treated with empty PLGA nanoparticles (np Empty) and mice treated with ALINO73-loaded nanoparticles (np ALINO). PMN infiltrating liver parenchyma (Extravasated PMN, white bars) or in centrolobular veins (PMN in vessels, light blue bars) were distinguished. Results are expressed in number of PMN per field of necrosis (magnification ×400) as mean ± SEM. Statistical test: Mann-Whitney *U*, significance is defined by $p < 0.05$. Statistical significances are indicated. (F) Histogram representing liver expression of KC mRNA 20 h after reperfusion in mice treated with empty PLGA nanoparticles (np Empty) and mice treated with ALINO73-loaded nanoparticles (np ALINO). Results are expressed in RU as mean ± SEM. Statistical test: Mann-Whitney *U*, significance is defined by $p < 0.05$. Statistical significances are indicated. (G) Representative ICAM-1 immunostainings of livers harvested from mice that underwent liver IR and were treated with empty nanoparticles (np Empty, left panel) or with np ALINO (right panel). IR, ischemia reperfusion; KC, keratinocyte chemoattractant; PLGA, poly(lactic-co-glycolic acid); PMN, polymorphonuclear neutrophils; RU, relative units.

improvement was associated with a lower liver expression of KC mRNA and lower infiltration of PMNs into the liver parenchyma, whereas the PMN number in centrolobular vessels was unchanged (Fig. 7E–F). The expression of ICAM-1 in the liver was reduced after treatment with np ALINO, as observed using immunohistochemistry (Fig. 7G).

Discussion

We have demonstrated in this study that the NOD1 pathway modulates liver IR injury through the induced expression of adhesion molecules. These adhesion molecules are mainly ICAM-1 and VCAM-1 and are expressed on LSECs as well as on hepatocytes. With an exploratory experiment using NOD1 antagonist-loaded nanoparticles, we strongly suggest that targeting NOD1 *in vivo* can reduce liver IR injury in part by reducing the expression of ICAM-1 in the liver.

NOD1 has been previously shown to impact liver IR through increased CD11b expression in PMNs.[18] However, the role of the NOD1 pathway in the liver, and more specifically the expression of adhesion molecules on hepatocytes and the endothelium was unknown. Numerous studies have demonstrated the clear impact of adhesion molecules, especially on the endothelium for the regulation of histological lesions and PMN tissue infiltration.[14,27,28] Our study emphasizes the role of NOD1 on adhesion molecule expression in the pathophysiology of liver IR. Indeed, ICAM-1 and VCAM-1 expression were increased upon NOD1 agonist treatment during liver IR. This upregulation of adhesion molecules in the whole liver and hepatocytes occurred within the first hours of reperfusion, before necrosis and PMN infiltration. This early expression of adhesion molecules is then probably a part of the first steps of pathophysiological mechanisms at the origin of reperfusion lesions.

At a cellular level, and more precisely in the context of *in vitro* culture of endothelial cells, E-selectin in addition to ICAM-1 and VCAM-1 is largely expressed and modulated after NOD1 pathway activation. However, the absence of significant induction of E-selectin expression after NOD1 activation at the whole organ level suggests that the endothelium is not the exclusive actor of expression of adhesion molecules in the liver.

The *ex vivo* and *in vitro* experiments demonstrate that hepatocytes are able to express ICAM-1 and VCAM-1 and these last are inducible upon NOD1 agonist treatment. Other adhesion molecules (CD44, P-selectin, PECAM) have been screened on hepatocytes, but with no significant modulation of their expression by NOD1 agonist (data not shown).

Although it is central, the PMN/hepatocyte interaction during IR has not been as extensively investigated as the PMN/endothelial interaction. During warm/cold ischemia, endothelial tissue is injured,[29] sinusoidal endothelial cells are detached and sloughed into the sinusoid lumen,[30] allowing PMNs direct access to hepatocytes[31,32] as confirmed by our analysis by electron microscopy (Fig. S4). We then designed a co-culture experiment to model the PMN/hepatocyte interface and clarify the hepatocellular role of NOD1 activation in this interaction. Electron microscopy analysis of our model confirmed the direct interaction between both cell types leading to hepatocyte death. Quantification of LDH shows that activation of NOD1 in the hepatocyte increases hepatocellular death upon PMN binding. The results of the interaction between *Nod1* KO hepatocyte and PMNs suggest that blocking hepatocyte NOD1 could prevent PMN-induced hepatocyte death *in vitro*.

In relation to the intracellular pathway, the effect of NOD1 appeared mediated through ERK and p38 phosphorylation in hepatocytes. The regulatory effect of ERK and p38 inhibitors confirms the role of the MAPK pathway in NOD1-mediated ICAM-1 and VCAM-1 expression. These findings support data obtained in other cell types such as PMNs.[18,19]

NOD1 is expressed widely in many organs and cell types.[33] The clinical potential of NOD1 antagonists could be extended to other organs such as renal IR pathogenesis[34] or myocardium infarct.[35] In the kidney, *Nod1* deficient mice are partially protected from IR-induced kidney injury. NOD1 activation by diaminopimelic acid worsens cardiac IR injury through p38 MAPK. *Nod1* knockdown using siRNA in cardiomyocytes attenuates cell death. The role of NOD1 in innate immune cells suggests that NOD1 antagonists should be evaluated for sepsis[36] or PMN-related hepatitis (*i.e.* alcoholic hepatitis).[37–39] The present results can serve as a basis for future studies investigating the therapeutic potential of NOD1 antagonists.

Our results and previous studies performed in the liver[18,19] strongly support evaluating the proof of concept for the use of NOD1 antagonists to prevent liver IR injury. Previous screening of chemical libraries on NOD receptors[20] led us to choose 2 prototypic NOD1 inhibitors from 2 different chemical entities based on their optimal IC50: ML130 and ALINO73 with the greatest inhibitory effect (Fig. S3). ML130 and ALINO73 are insoluble in aqueous solutions and insufficiently soluble in non-toxic hydrophobic solvents. Because these low hydrophilic properties prevented their use *in vivo,* we used nanoparticles to transport insoluble NOD1 antagonists to the liver.[40] We choose PLGA nanoparticles because of their high biocompatibility and FDA approved safety. PLGA is currently used in several drugs such as: Sandostatin LAR© (USAN (United States Adopted Name): Octreotide)[41] for neuroendocrine tumors, Bydureon© (USAN: Exenatide)[42] in diabetes and Risperdal Consta© (USAN: Risperidone) in schizophrenia.[43]

The *in vitro* testing of PLGA nanoparticles loaded with ML130 or ALINO73 showed that np ML130 was not effective while np ALINO inhibited NOD1 activity at least as efficiently as free ALINO73 suggesting a high bioavailability despite the PLGA integration. In mice, this NOD1 antagonist-loaded nanoparticle, np ALINO, decreased the area of necrosis induced by liver IR by about 40%. This decrease in histological lesions was associated with a 33% decrease in serum aminotransferase, supporting the potential role of np ALINO as a therapeutic approach to prevent liver IR. The np ALINO treatment was also associated with lower KC mRNA expression in the liver, lower PMN infiltration and reduced ICAM expression. The reduction of KC expression could have reduced the total number of PMNs recruited to the liver. Indeed, np ALINO did not impact the number of PMNs in centrolobular vessels, but significantly reduced the severity of PMN infiltration in necrosis areas. These results raise the therapeutic potential of NOD1 antagonists in preventing hepatic IR in humans. The use of NOD1 antagonists should be tested during different steps of liver transplantation. These NOD1 antagonists could be used either in the donor before the organs are harvested, or added to the preservation protocol, as well as a treatment during reperfusion in the recipient.

In conclusion, this study states that NOD1 regulates adhesion molecule expression in the liver. NOD1 activation and blockage experiments confirm that the NOD1 pathway modulates the severity of liver IR injury. These data complement the impact of NOD1 on PMN function and migration. Thus, NOD1 has a dual role and targets 2 different actors implicated in reperfusion injury. However, the relative contribution of each actor (PMN or adhesion molecule) on liver IR injury is unclear. New experiments are needed to puzzle out the full mechanism by which the NOD1 pathway exerts this effect. This work supports the development of NOD1 inhibitors.

Financial support

The author acknowledges funding support from the National Institute on Alcohol Abuse and Alcoholism grant 1U01AA021908, AFEF, program StartAIRR ANOD1 Region Haut de France.

Conflict of interest

The authors declare no conflict of interest in relation to this manuscript.

Please refer to the accompanying ICMJE disclosure forms for further details.

Authors' contributions

E.G., M.B.S., L.D., G.L., F.A., F.M., C.G., P.M. and M.N. generated data, L.D., G.L., S.D. and Ph.M. designed experiments; V.G. performed histological analysis; N.L.C., R.C., B.B., D.B. designed and provided essential tools; L.D., G.L., A.L. analyzed the data; L.D., G.L., N.L.C., R.C. prepared the manuscript; A.L., S.D., F.A. and Ph.M. edited the manuscript; L.D., G.L. and Ph.M. provided experimental funding.

Acknowledgements

Authors would like to thank Nathalie Jouy, Anne Loyens and Meryem Tardivel from the Flow Core Facility – BioImaging Center Lille (F-59000 Lille, France) for the access and excellent technical support. Thanks to Melanie Legrand, Cyril Degraeve, Amélie Mine, Emeline Gorecki, Justine Beauchamp, Mélanie Bollier, Perrine Six and Arnaud Dendooven for technical assistance.

Supplementary data

Supplementary data to this article can be found online at https://doi.org/10.1016/j.jhep.2019.01.019.

References

[1] Casavilla A, Ramirez C, Shapiro R, Nghiem D, Miracle K, Bronsther O, et al. Experience with liver and kidney allografts from non-heart-beating donors. Transplantation 1995;59:197–203.
[2] Clavien PA, Harvey PR, Strasberg SM. Preservation and reperfusion injuries in liver allografts. An overview and synthesis of current studies. Transplantation 1992;53:957–978.
[3] Jaeschke H. Mechanisms of Liver Injury. II. Mechanisms of neutrophil-induced liver cell injury during hepatic ischemia-reperfusion and other acute inflammatory conditions. Am J Physiol Gastrointest Liver Physiol 2006;290:G1083–G1088.
[4] Lentsch AB, Kato A, Yoshidome H, McMasters KM, Edwards MJ. Inflammatory mechanisms and therapeutic strategies for warm hepatic ischemia/reperfusion injury. Hepatology 2000;32:169–173.
[5] Serracino-Inglott F, Habib NA, Mathie RT. Hepatic ischemia-reperfusion injury. Am J Surg 2001;181:160–166.
[6] Lee DD, Singh A, Burns JM, Perry DK, Nguyen JH, Taner CB. Early allograft dysfunction in liver transplantation with donation after cardiac death donors results in inferior survival. Liver Transpl 2014;20:1447–1453.
[7] Merion RM, Pelletier SJ, Goodrich N, Englesbe MJ, Delmonico FL. Donation after cardiac death as a strategy to increase deceased donor liver availability. Ann Surg 2006;244:555–562.
[8] Peralta C, Jimenez-Castro MB, Gracia-Sancho J. Hepatic ischemia and reperfusion injury: effects on the liver sinusoidal milieu. J Hepatol 2013;59:1094–1106.
[9] Jaeschke H. Molecular mechanisms of hepatic ischemia-reperfusion injury and preconditioning. Am J Physiol Gastrointest Liver Physiol 2003;284:G15–G26.
[10] Glanemann M, Langrehr JM, Stange BJ, Neumann U, Settmacher U, Steinmuller T. Clinical implications of hepatic preservation injury after adult liver transplantation. Am J Transplant 2003;3:1003–1009.
[11] Springer TA. Adhesion receptors of the immune system. Nature 1990;346:425–434.
[12] Caldwell-Kenkel JC, Thurman RG, Lemasters JJ. Selective loss of non-parenchymal cell viability after cold ischemic storage of rat livers. Transplantation 1988;45:834–837.
[13] Steinhoff G, Behrend M, Schrader B, Pichlmayr R. Intercellular immune adhesion molecules in human liver transplants: overview on expression patterns of leukocyte receptor and ligand molecules. Hepatology 1993;18:440–453.
[14] Ala A, Dhillon AP, Hodgson HJ. Role of cell adhesion molecules in leukocyte recruitment in the liver and gut. Int J Exp Pathol 2003;84:1–16.
[15] Benkoel L, Dodero F, Hardwigsen J, Benoliel AM, Bongrand P, Botta-Fridlund D, et al. Expression of intercellular adhesion molecule-1 (ICAM-1) during ischemia-reperfusion in human liver tissue allograft: image analysis by confocal laser scanning microscopy. Dig Dis Sci 2003;48:2167–2172.
[16] Lu L, Zhou H, Ni M, Wang X, Busuttil R, Kupiec-Weglinski J, Zhai Y. Innate immune regulations and liver ischemia-reperfusion injury. Transplantation 2016;100:2601–2610.
[17] Jaeschke H. Reactive oxygen and mechanisms of inflammatory liver injury: Present concepts. J Gastroenterol Hepatol 2011;26(Suppl 1): 173–179.
[18] Dharancy S, Body-Malapel M, Louvet A, Berrebi D, Gantier E, Gosset P, et al. Neutrophil migration during liver injury is under nucleotide-binding oligomerization domain 1 control. Gastroenterology 2010;138: 1546–U1421.
[19] Scott MJ, Chen C, Sun Q, Billiar TR. Hepatocytes express functional NOD1 and NOD2 receptors: a role for NOD1 in hepatocyte CC and CXC chemokine production. J Hepatol 2010;53:693–701.
[20] Rickard DJ, Sehon CA, Kasparcova V, Kallal LA, Haile PA, Zeng X, et al. Identification of selective small molecule inhibitors of the nucleotide-binding oligomerization domain 1 (NOD1) signaling pathway. PLoS One 2014;9 e96737.
[21] Khan PM, Correa RG, Divlianska DB, Peddibhotla S, Sessions EH, Magnuson G, et al. Identification of inhibitors of NOD1-induced nuclear factor-κB activation. ACS Med Chem Lett 2011;2:780–785.
[22] Yamashita T, Ishibashi Y, Nagaoka I, Kasuya K, Masuda K, Warabi H, et al. Studies of glycogen-induced inflammation of mice. Dynamics of inflammatory responses and influence of antiinflammatory drugs and protease inhibitors. Inflammation 1982;6:87–101.
[23] Seglen PO. Preparation of isolated rat liver cells. Methods Cell Biol 1976;13:29–83.
[24] Koressaar T, Remm M. Enhancements and modifications of primer design program Primer3. Bioinformatics 2007;23:1289–1291.
[25] Untergasser A, Cutcutache I, Koressaar T, Ye J, Faircloth BC, Remm M, et al. Primer3–new capabilities and interfaces. Nucleic Acids Res 2012;40 e115.
[26] Le Broc-Ryckewaert D, Carpentier R, Lipka E, Daher S, Vaccher C, Betbeder D, et al. Development of innovative paclitaxel-loaded small PLGA nanoparticles: study of their antiproliferative activity and their molecular interactions on prostatic cancer cells. Int J Pharm 2013;454:712–719.
[27] Eltzschig HK, Eckle T. Ischemia and reperfusion–from mechanism to translation. Nat Med 2011;17:1391–1401.
[28] Zhai Y, Petrowsky H, Hong JC, Busuttil RW, Kupiec-Weglinski JW. Ischaemia-reperfusion injury in liver transplantation–from bench to bedside. Nat Rev Gastroenterol Hepatol 2013;10:79–89.
[29] Selzner N, Rudiger H, Graf R, Clavien PA. Protective strategies against ischemic injury of the liver. Gastroenterology 2003;125:917–936.
[30] Gao W, Bentley RC, Madden JF, Clavien PA. Apoptosis of sinusoidal endothelial cells is a critical mechanism of preservation injury in rat liver transplantation. Hepatology 1998;27:1652–1660.
[31] Jaeschke H, Farhood A, Smith CW. Neutrophils contribute to ischemia/reperfusion injury in rat liver in vivo. FASEB J 1990;4:3355–3359.
[32] Imamura H, Brault A, Huet PM. Effects of extended cold preservation and transplantation on the rat liver microcirculation. Hepatology 1997;25:664–671.
[33] Philpott DJ, Sorbara MT, Robertson SJ, Croitoru K, Girardin SE. NOD proteins: regulators of inflammation in health and disease. Nat Rev Immunol 2014;14:9–23.
[34] Shigeoka AA, Kambo A, Mathison JC, King AJ, Hall WF, da Silva Correia J, et al. Nod1 and nod2 are expressed in human and murine renal tubular epithelial cells and participate in renal ischemia reperfusion injury. J Immunol 2010;184:2297–2304.
[35] Yang H, Li N, Song LN, Wang L, Tian C, Tang CS, et al. Activation of NOD1 by DAP contributes to myocardial ischemia/reperfusion injury via multiple signaling pathways. Apoptosis 2015;20:512–522.
[36] Cartwright N, Murch O, McMaster SK, Paul-Clark MJ, van Heel DA, Ryffel B, et al. Selective NOD1 agonists cause shock and organ injury/dysfunction in vivo. Am J Respir Crit Care Med 2007;175:595–603.
[37] Takahashi T, Kamimura T, Ichida F. Ultrastructural findings on polymorphonuclear leucocyte infiltration and acute hepatocellular damage in alcoholic hepatitis. Liver 1987;7:347–358.
[38] Taieb J, Delarche C, Paradis V, Mathurin P, Grenier A, Crestani B, et al. Polymorphonuclear neutrophils are a source of hepatocyte growth factor in patients with severe alcoholic hepatitis. J Hepatol 2002;36:342–348.
[39] Lazaro R, Wu R, Lee S, Zhu NL, Chen CL, French SW, et al. Osteopontin deficiency does not prevent but promotes alcoholic neutrophilic hepatitis in mice. Hepatology 2015;61:129–140.
[40] Park JK, Utsumi T, Seo YE, Deng Y, Satoh A, Saltzman WM, et al. Cellular distribution of injected PLGA-nanoparticles in the liver. Nanomedicine 2016;12:1365–1374.
[41] Zhang Y, Sophocleous AM, Schwendeman SP. Inhibition of peptide acylation in PLGA microspheres with water-soluble divalent cationic salts. Pharm Res 2009;26:1986–1994.
[42] Qi F, Wu J, Hao D, Yang T, Ren Y, Ma G, et al. Comparative studies on the influences of primary emulsion preparation on properties of uniform-sized exenatide-loaded PLGA microspheres. Pharm Res 2014;31:1566–1574.
[43] Rawat A, Bhardwaj U, Burgess DJ. Comparison of in vitro-in vivo release of Risperdal((R)) Consta((R)) microspheres. Int J Pharm 2012;434: 115–121.